Author Manuscript

Author Manuscript

Author Manuscript

Author Manuscript

HHS Public Access

Author manuscript

J Toxicol Environ Health A. Author manuscript; available in PMC 2015 March 23.

Published in final edited form as:

J Toxicol Environ Health A. 2013 ; 76(16): 953–972. doi:10.1080/15287394.2013.826567.

BIOLOGICAL RESPONSE TO NANO-SCALE TiO_2: ROLE OF PARTICLE DOSE, SHAPE AND RETENTION

Rona M. Silva[1], **Christel TeeSy**[1], **Lisa Franzi**[2], **Alex Weir**[3], **Paul Westerhoff**[3], **James E. Evans**[4,5], and **Kent E. Pinkerton**[1,*]

[1]Center for Health and the Environment, University of California Davis, Davis, CA 95616

[2]Department of Pulmonary and Critical Care Medicine, CCRBM, School of Medicine, University of California Davis, Davis, CA 95616

[3]School of Sustainable Engineering and The Built Environment, Arizona State University, Tempe, AZ 85287

[4]Department of Molecular and Cellular Biology, University of California, Davis, CA 95616

[5]Pacific Northwest National Laboratory, Environmental Molecular Sciences Laboratory, Richland, WA 99354

Abstract

TiO_2 is one of the most widely used nanomaterials, valued for its highly refractive, photocatalytic and pigmenting properties. TiO_2 is also classified by the International Agency for Research on Cancer (IARC) as a possible human carcinogen. The objectives of this study were to establish a lowest observed effect level (LOEL) for nano-scale TiO_2, determine TiO_2 uptake in the lungs, and estimate toxicity based on physico-chemical properties and retention in the lungs. *In vivo* lung toxicity of nano-scale TiO_2 using varying forms of well-characterized, highly-dispersed TiO_2 was assessed. Anatase/rutile P25 spheres (TiO_2-P25), pure anatase spheres (TiO_2-A), and anatase nanobelts (TiO_2-NB) were tested. To determine the effects of dose and particle characteristics, male Sprague-Dawley rats were given TiO_2 (0, 20, 70, or 200 μg) via intratracheal instillation. Broncho-alveolar lavage fluid (BALF) and lung tissue were obtained for analysis 1 and 7 days post exposure. Despite abundant TiO_2 inclusions in all exposed animals, only TiO_2-NB elicited any significant degree of inflammation seen in BALF at the 1-day time-point. This inflammation resolved by 7 days; although, TiO_2 particles had not cleared from alveolar macrophages recovered from the lung. Histological examination showed TiO_2-NB caused cellular changes at day 1 which were still evident at day 7. We conclude TiO_2-NB is the most inflammatory with a lowest observable effect level of 200 μg at 1 day post instillation.

Keywords

Titanium dioxide particles; pulmonary toxicity; inflammation; lung dosimetry; engineered nanomaterial

*Correspondence: Dr. Kent E. Pinkerton, Center for Health and the Environment, University of California, One Shields Avenue, Davis, CA 95616. Tel: (530) 752-8334. kepinkerton@ucdavis.edu.

Author Manuscript Author Manuscript Author Manuscript Author Manuscript

INTRODUCTION

Titanium dioxide (TiO_2) is one of the most widely used nano-scale materials to date, yet it is also classified by the International Agency for Research on Cancer (IARC) as a possible carcinogen to humans. Valued for its highly-refractive, photocatalytic and pigmenting properties, the conversion of bulk to nano-scale TiO_2 for consumer products (e.g. topical sunscreens and cosmetics) and industrial products (e.g. paints and coatings) is rapidly increasing (Robichaud et al. 2009). Thus, there is high probability for TiO_2 exposure, especially in the workplace based on mass production and inhalation exposure scenarios (Kuhlbusch et al. 2011).

Investigators report conflicting results regarding TiO_2 toxicity. Nano-scale TiO_2 has been observed to cause pulmonary inflammation in rats and mice *in vivo* (Bonner et al. 2013; Hougaard et al. 2010; Ma-Hock et al. 2009; McKinney et al. 2012; Warheit et al. 2006), and a number of *in vitro* studies suggest that TiO_2 engineered nanomaterials can elicit oxidative stress and DNA damage (Cui et al. 2012; Meena et al. 2012). It has been postulated nano-TiO_2 can cross the placental barrier resulting in reduced daily sperm production (Takeda et al. 2009) and altered neurological development (Hougaard et al. 2010; Shimizu et al. 2009; Takeda et al. 2009) in exposed offspring. However, there are a number of studies demonstrating no adverse pathology associated with TiO_2 exposure. For example, Horie et al. did not find lung inflammation or oxidative stress in rats exposed intratracheally to fine or nano-scale TiO_2 (2012), and Saber et al. did not find DNA damage after instillation of nano-scale TiO_2 (2012).

The lack of congruent findings across nano-scale TiO_2 studies is challenging for regulators charged with the task of protecting health and welfare because promulgation of exposure standards requires predictable dose-response patterns proven reliable by multiple studies. The objectives of the present study are to establish a lowest observed effect level (LOEL) for nano-scale TiO_2 and better understand TiO_2 nano-scale toxicity based on physico-chemical characteristics and retention. Three different forms of well characterized, highly dispersed TiO_2 nanoparticles, anatase/rutile P25 spheres (TiO_2-P25), pure anatase spheres (TiO_2-A), and anatase nanobelts (TiO_2-NB), were intratracheally instilled into the lungs of adult male Sprague Dawley rats. Acute lung toxicity was evaluated 1 and 7 days post exposure. LOEL was determined with doses ranging from 0–200 μg since several *in vivo* studies show intratracheal instillation of nano-scale TiO_2 at a dose of ~1 mg/kg of bodyweight causes acute pulmonary inflammation (Nemmar, Melghit, and Ali 2008; Rehn et al. 2003; Renwick et al. 2004; Sager, Kommineni, and Castranova 2008; Warheit, Webb, Reed, et al. 2007). The dose ranged from 0–0.5 mg/kg of bodyweight per adult male Sprague Dawley rat (~0.4 kg). Inflammation and particle retention with time post-exposure were compared among the three types of nanoparticles. We hypothesized that the physico-chemical particle characteristics of TiO_2 (e.g. shape, phase and structure) modulate the dose-dependent inflammation and cellular injury observed in the respiratory tract.

Author Manuscript Author Manuscript Author Manuscript Author Manuscript

METHODS

Physicochemical Characterization of TiO_2 Nanoparticles

A full description of the physico-chemical characterization of the three forms of TiO_2 nanoparticles has been recently described by Xia and colleagues (2012). Three distinct TiO_2 forms, anatase/rutile P25 spheres (TiO_2-P25), pure anatase spheres (TiO_2-A), and anatase nanobelts (TiO_2-NB), were tested. TiO_2-P25 (81% anatase and 19% rutile) were obtained from Evonik (Parsippany, NJ). Flame Aerosol Reactor (FLAR)-synthesized TiO_2-A were provided by Dr. Pratim Biswas (Department of Energy, Environmental & Chemical Engineering, Washington University, St. Louis, MO). TiO_2-NB were attained from the laboratory of Dr. Nianqiang Wu (Mechanical and Aerospace Engineering, West Virginia University, Morgantown, WV), as described previously (Hamilton et al. 2009). Scanning electron microscope (SEM) images of all three particle types are illustrated in Figure 1. Surface area measured by BET (Brunauer, Emmett, & Teller) was 53, 173, and 18 m^2/g for TiO_2-P25, TiO_2-A, and TiO_2-NB, respectively. The specific TiO_2 forms were chosen for analysis because P25 has been used as the *de facto* standard titania photocatalyst and reported in more than one thousand papers since 1990 (Ohtani 2010). Furthermore, TiO_2 toxicity is thought to increase with anatase content (Warheit, Webb, Reed, et al. 2007) and aspect ratio (Hamilton et al. 2009).

Animal Protocol

Outbred male Sprague-Dawley rats (Harlan Laboratories, Inc., Hayward, CA), 9–10 weeks of age, were used for all experiments. Sprague-Dawley rats were selected based on their extensive use in experimental studies, ease in handling, and high tolerance to intratracheal instillation procedures. Upon arrival, animals were weighed and housed in pairs, in plastic cages (~20” × 16” × 8 ¼”) with narrow, straight-wire, stainless steel lids, enrichment objects, and CareFRESH® absorptive paper bedding. Animals were acclimated for one week and given access *ad libitum* to a standard commercial, block-type food and water throughout the duration of the experiment. Animal bedding was replaced and cages were changed on a weekly basis. Aseptic animal rooms were maintained at 22°C with 12-hour dark/light cycles.

Animal weights were recorded throughout the study. Prior to exposure, animals were assigned to treatment groups by weight. This was done in a manner ensuring the mean weight for all treatment groups for day and particle type was statistically the same. Sentinel rats were maintained in the same room and tested to ensure experimental animals remained free of pathogens and/or parasites. UC Davis Institutional Animal Care and Use Committee (IACUC) approval was obtained for all procedures involving rats in this study.

Preparation of TiO_2 Suspensions

Dry TiO_2 nanoparticle stock samples were stored in a desiccator under aseptic conditions at room temperature until needed. All solid-phase TiO_2 used for the nanoparticle suspensions were measured using a calibrated, analytical microbalance with a minimum limit of detection equal to 0.003 mg (M5P Filter Microbalance, Sartorius, Goettingen, Germany). TiO_2 engineered nanomaterials were suspended in dispersion media (DM) prepared as

Author Manuscript Author Manuscript Author Manuscript Author Manuscript

previously described (Porter et al. 2008). This media was chosen for its similarity to the endogenous fluid of the lung, and its ability to effectively disperse and prevent agglomeration of similar TiO_2 particles without affecting particle toxicity. To summarize, distearoylphosphatidylcholine (DSPC: Sigma-Aldrich), low-endotoxin rat serum albumin (Sigma-Aldrich), 0.9% sterile saline, and 100% ethanol were used to make the DM. Though dipalmitoylphosphatidylcholine (DPPC) was used by Porter, and distearoylphosphatidylcholine (DSPC) was used herein, the two are similar membrane lipids that contain two saturated symmetric hydrocarbon chains. The main difference is that DPPC has a C16 carbon tail, and DSPC has a C18 carbon tail. Because it is the choline group present on both molecules that is charged and acts as the surfactant, the two were essentially interchangeable for our purposes. Proportions were such that in 1 mL of DM there were 0.399 mL of sterile saline, 0.600 mL of rat serum albumin (1 mg RSA powder:1 mL 0.9% saline), and 0.001 mL of DSPC (10 mg DSPC powder: 1 mL ethanol). Suspensions of the highest dose (200μg/250μL) were created by adding DM to a Falcon™ tube with a known mass of TiO_2-P25, TiO_2-A, or TiO_2-NB. Suspensions of spherical TiO_2 were probe-sonicated (Qsonicca, LLC, Newton, CT) for 30 minutes using a 10-second on/off duty cycle to ensure adequate particle dispersal. TiO_2 nanobelt suspensions were continuously stirred for 30 minutes with a magnetic micro stir bar to prevent breakage of the delicate structures. Direct dilutions of the 200 μg/250μL suspensions were done with DM to make lower dose suspensions of TiO_2 spheres (10 and 70 μg/250μL) as well. These dilutions were also sonicated using the aforementioned protocols. TiO_2 nanobelts were tested only at the highest dose due to constraints on animal supply and time. The DM alone served as the sham control instillate. To assess potential passivation of particles by the dispersion media, high-dose (200 μg/250μL) suspensions of TiO_2 in phosphate buffered saline (PBS), and sterile 0.9% saline were made for comparisons to PBS, and saline sham controls, respectively, and to high-dose TiO_2 suspensions in DM. All suspensions were prepared and loaded into 1cc Monoject ®syringes fitted with 1.5 inch, 22 gauge, blunt-tipped Monoject® needles directly before instillation. Sonication, syringe loading, and instillation were timed to ensure the highest degree of particle dispersion.

Intratracheal Instillation

Food was removed from the animal cages two hours prior to instillation. Each animal was placed in a plexiglass anesthesia chamber and exposed to gaseous Isoflurane for 2 minutes at a rate of 1 liter/minute. Once an animal was sufficiently sedated, it was removed from the chamber and instilled with 0, 10, 70 or 200 μg of TiO_2 using an intratracheal instillation board. Care was taken to deliver the instillate upon the inhalation breath to enhance uniform particle delivery to the lungs. Animals were returned to their cages and allowed to recover with free access to food and water. During recovery, animals were monitored for any signs of distress. For each TiO_2 type, a sample size of 48 rats was used, with six animals per dose (including controls) and 24 rats per time-point (1 and 7 days post-exposure).

Collection and Analysis of BALF and Lung Tissue Samples

Animals were weighed and euthanized with an intraperitoneal injection of Beuthanasia-D (65 mg/kg) at 1 or 7 days post TiO_2 exposure. Broncho-alveolar lavage (BAL) was then performed. Briefly, the trachea was cannulated with a 16-gauge cannula. Five separate 5 mL

Author Manuscript Author Manuscript Author Manuscript Author Manuscript

aliquots of 0.9% sterile saline were slowly instilled into the lungs using a single 6 mL Monoject® syringe. Aliquots one and two were combined in a single 15 mL Falcon™ tube; while, aliquots three to five were combined in a 50 mL Falcon™ tube. Tubes were centrifuged at 4°C and 2000 rpm for 10 minutes (Beckman Coulter, Inc.). Supernatant from the 15 mL Falcon™ tube was collected for same-day protein and LDH analyses, which were performed using kits from Thermo Scientific (Rockford, IL) and Sigma-Aldrich (St. Louis, MO), respectively. The supernatant from the 50 mL Falcon™ tube was discarded. Cells from the 15 mL Falcon™ tube were resuspended in 10 mL 0.9% sterile saline and combined with those of the 50 mL Falcon™ tube for determination of total cell numbers and cell viability with a hemocytometer and Trypan Blue exclusion dye, respectively. Cell differentials and particle uptake/retention (i.e. visible TiO_2 inclusions in macrophages) were determined by Brightfield microscopy by counting a minimum of 500 cells from a 100 mL cytospin slide stained with Diff Qwik® (Dade Behring Inc., Newark, DE). Blind analysis was completed by one individual and then compared to results obtained by a second person with similar training to ensure minimal observer bias.

In addition to BALF, histological samples were collected from each animal. After the whole lung was lavaged for BALF collection, the right lobes were tied off with surgical thread and removed. Each right lobe was frozen at −80°C in a separate NUNC™ cryovial for inductively-coupled plasma mass spectrometry (ICP-MS) analysis and/or other future assays. The left lung was fixed hydrostatically (30 cm) using 4% paraformaldehyde (PF) for one hour then stored in the same fixative. After 48 hours, tissue stored in buffered formalin was micro-dissected such that two complimentary halves representing the mediastinal and intercostal portions of the lung were prepared. Airway generations along the main axial pathway were mapped, and approximately six transverse slices (proximal to distal) were made starting from the lobar bronchus. Tissue slices were then dehydrated in a series of graded ethanol, embedded in paraffin, and sectioned to 5 μm with a microtome (HM 355, Microm, Walldorf, Germany). Lung sections were placed on slides, stained with hematoxylin (Harris Hematoxylin, American MasterTech, Lodi, CA) and eosin (Eosin Y Stain, American MasterTech, Lodi, CA), and coverslipped for observations using Brightfield microscopy. Histopathological evaluations were made of cellular changes and inflammation for all regions of the lungs with special emphasis on the examination of terminal bronchioles, bronchoalveolar duct junctions, and alveoli.

Total cell counts and cell differentials along with lactate dehydrogenase (LDH) and Bradford (protein) assays were performed on the BALF as they are common, relatively simple, and inexpensive tests for lung cytotoxicity. Brightfield microscopy of BAL cells and ICP-MS of tissue samples were used to determine TiO_2 retention in the lungs.

ICP Analysis

To pinpoint the region of the lungs with the greatest deposition/retention of particles, ICP-MS analysis was performed on right cranial and caudal lung lobes from the sham control and 200 μg TiO_2 instillation exposures. Particle loading was compared between the cranial lobe and caudal lobe because they represent short and long airway paths of the lung, respectively. ICP-MS allowed for highly sensitive and precise detection of TiO_2; the limit of

Author Manuscript Author Manuscript Author Manuscript Author Manuscript

detection was 600 ng of titanium. ICP-MS procedures were similar to those previously applied for analysis of titanium content in food, personal care products and paints (Weir et al. 2012). Complete details for digesting titanium dioxide in lung tissues is described elsewhere (Weir 2011). Briefly, tissues were weighed and dried at 80°C until weight loss ceased (~12–18 hours). Subsequently, a microwave digestion method using high purity nitric and hydrofluoric acids was implemented to digest lung tissues and other organic matrices. Next, the liquid portion of each sample was evaporated using a hotplate (160°C, 3–4 hours), leaving only TiO_2, which was re-suspended in a dilute nitric acid solution for ICP-MS analysis. ICP-MS results were subsequently confirmed by ICP-optical emission spectrometry (OES).

Statistical Analysis

Data are presented as mean ± standard error of the mean (SEM). JMP statistical software (Cary, NC) was used to perform analysis of variance (ANOVA) and post hoc Tukey's tests, or Wilcoxon pair-wise comparisons with a significance level of $p \leq 0.05$. The analyses considered the main effects of and interactions between the variable factors of dose, time, and particle type. The data were analyzed for deviations from the assumptions of ANOVA; no outliers were identified via box plots.

RESULTS

Animal weight

Animal weight was unaffected by intratracheal instillation of the three tested TiO_2 forms compared to controls (data not shown). For animals exhibiting inflammation, there was no correlation between weight change following instillation and subsequent degree of inflammation post exposure (data not shown).

Toxic effects as determined with BALF

Total cell counts in BALF were similar between control and TiO_2 exposed animals, regardless of the dose or TiO_2 form (data not shown). While a dose-response for the percentage of BALF neutrophils was not found following exposure to the spherical TiO_2 nanoparticles, TiO_2-P25 and TiO_2-A, exposure to TiO_2-NB resulted in a significantly increased percent of BALF neutrophils 1-day post exposure at the highest dose (200 μg) compared to the control (Figure 2). However, by 7 days post exposure, BALF neutrophils had returned to control values.

While not resulting in toxicity as reflected by BALF, TiO_2 inclusions were seen in BAL macrophages of TiO_2-P25 and TiO_2-A exposed rats (Figure 3), suggesting that the nanospheres reached the deep lung. The percentage of macrophages containing visible inclusions ranged from approximately 0.5 to 20 percent in animals exposed to TiO_2-P25 or TiO_2-A (Figure 4, top vs bottom panels, respectively) remaining fairly stable from 1 to 7 days post exposure (Figure 4, left panels vs. right panels, respectively). While TiO_2-NB inclusions were found in BAL macrophages (Figure 3), the percentage of inclusions was not quantified because it was very difficult to consistently identify the delicate, fibrillar TiO_2-

Author Manuscript Author Manuscript Author Manuscript Author Manuscript

NB structures with Brightfield microscopy; however, retention by macrophages was confirmed by TEM(Figure 5).

Total protein and LDH assays showed no significant differences between control and exposed animals (data not shown). Statistical comparisons of percent PMN and total cell data from animals exposed to 200 μg/250 μL of TiO_2 in PBS, sterile saline, and DM also showed no significant differences due to suspension media (data not shown).

Changes in the lung parenchyma

At 1 day post exposure, animals instilled with 200 μg of TiO_2 exhibited focal centriacinar bronchiolitis/alveolitis often in regions near visible particle agglomerates, or particle-laden macrophages in the air spaces (Figure 6). Qualitative assessment suggested TiO_2-NB caused a greater effect than either of the spherical TiO_2 nanoparticles. This is especially evident in the regions surrounding blood vessels, where heavy inflammatory infiltrates can be seen entering the airspaces (Figure 7, left). By day 7, inflammation appeared to decrease in animals exposed to TiO_2-P25 or TiO_2-A even though particles were still present in the alveoli. However, inflammatory infiltrates, and macrophages in the air spaces were abundantly visible at 7 days, in animals exposed to TiO_2-NB (Figure 7, right).

Lung burden of TiO_2 by ICP

When normalized to lung lobe mass, the cranial lobe was found to have less of all three TiO_2 forms compared to the caudal lobe at both 1 and 7 days post-exposure (Figure 6, top panel vs. bottom panel). These results reflect what was shown by microscopy; the lung retained TiO_2 nanoparticles 7 days after instillation. We feel confident about these results as over a detected concentration range of 0.06 to 0.35 μg TiO_2/L the correlation between ICP-MS and ICP-OES results was very high (R^2>0.99) with a linear slope within 6% of a one-to-one line.

DISCUSSION

The goal of this study was to assess the *in vivo* lung toxicity of nano-scale TiO_2 and determine a LOEL using three well characterized, highly dispersed TiO_2 forms. The three different forms of TiO_2 (anatase/rutile P25 spheres (TiO_2-P25), pure anatase spheres (TiO_2-A), and anatase nanobelts (TiO_2-NB)) were used to determine whether physico-chemical characteristics correlated to particle retention and/or inflammation. Instillation, rather than inhalation, was chosen as the route of exposure to precisely control dosimetry for LOEL determination. Despite alveolar macrophage TiO_2 inclusions being found for all three TiO_2 forms, only animals exposed to TiO_2-nanobelts (NB; highest dose of 200 μg) had a significantly greater percentage of neutrophils in BALF than control animals 1day post exposure; however, this resolved by 7days post-exposure. Due to lack of toxic response, a definite LOEL could not be determined for the TiO_2-P25 and TiO_2-A nanoparticles, although doses used are likely to be within a range of a worse-case exposure scenario in an occupational or environmental setting.

When taken with the sum of nano-scale TiO_2 research, results from this study mirror previous findings that not all TiO_2 engineered nanomaterials are equal in their ability to

Author Manuscript Author Manuscript Author Manuscript Author Manuscript

elicit toxicity. Many *in vivo* TiO_2 studies to date 1) present incomplete particle characterization; 2) use questionable suspension media for intratracheal instillation procedures; 3) compare particles with many inherent differences; and/or 4) do not provide dosimetric measurements when correlating pulmonary toxicity and particle exposure. This study is unique in its careful attempt to control for these potentially confounding issues. Results from this study do not show a correlation between nanoparticle persistence and inflammation for spherical anatase-containing TiO_2, which is contrary to other studies suggesting that anatase TiO_2 is pathogenic (Warheit, Webb, Reed, et al. 2007; Zhang J 2012). TiO_2-A had the largest surface area to mass ratio (173 m^2/g) of the three particles, and surface area has been correlated to increased inflammation in previous instillation (Oberdorster 2000; Oberdorster et al. 1992; Renwick et al. 2004; Saber, Jensen, et al. 2012) and inhalation studies (Bermudez et al. 2004; Oberdorster, Ferin, and Lehnert 1994).

Although TiO_2-P25 and TiO_2-A are clearly retained, this does not seem to influence neutrophilia. The single exposure may have insufficiently taxed the phagocytic defenses of the lung, or at these doses, TiO_2-P25 and TiO_2-A may not have reached the threshold surface area for eliciting inflammatory responses (Saber, Jacobsen, et al. 2012; Stoeger et al. 2006). Compared to the spherical TiO_2 nanoparticles, TiO_2-NB is an order of magnitude larger, fibrillar, and thus, has a high-aspect ratio. Research with asbestos and other high-aspect ratio nanoparticles shows impeded clearance from the lungs after inhalation exposure leading to the pathogenesis of diseases such as pulmonary fibrosis and mesothelioma (Bonner 2010). At present, there is evidence that high-aspect ratio TiO_2-NB are relatively more pathogenic, and may elicit "frustrated phagocytosis" by macrophages, lysosomal disruption, and impaired lung clearance (Donaldson et al. 2011; Hamilton et al. 2009). Indeed, long-term studies show a link between particle retention and pulmonary pathology (Bermudez et al. 2004; Oberdorster, Ferin, and Lehnert 1994).

Though relatively high bolus doses of TiO_2 (NIOSH recommends an average time-weighted concentration = 0.3 mg/m^3 during a 40-hr work week) were used in this study and delivered by intratracheal instillation, it is important to understand that this approach does not truly mimic real-world exposure conditions or deposition patterns in the lung that would occur via inhalation. Intratracheal instillation was chosen to simply evaluate how the physico-chemical particle characteristics and retention of a precise dose of TiO_2 nanoparticles affects the lung. Instilled doses were chosen based on previous research showing significant acute pulmonary inflammation after exposure to ≤ 1 mg/kg of TiO_2 (Nemmar, Melghit, and Ali 2008; Rehn et al. 2003; Renwick et al. 2004; Sager, Kommineni, and Castranova 2008; Warheit, Webb, Reed, et al. 2007). We attempted to discern a LOEL using doses ranging from 0–0.5 mg/kg of bodyweight, and found the chosen dose range was not appropriate for all the TiO_2 forms. Though we were unable to determine a LOEL for the spherical TiO_2 forms tested, we did find an inflammatory LOEL of 0.5 mg/kg (200 μg) for TiO_2-NB, at 1-day post instillation using significant increase in BALF neutrophils as the toxic endpoint. To establish a LOEL for TiO_2-P25 and TiO_2-A, higher doses should be more informative. Further, responses following more realistic inhalation exposures should be evaluated with all three of these TiO_2 types in order to derive other lowest and/or no-effect levels for purposes of risk characterization and further development of exposure standards. This is especially

Author Manuscript Author Manuscript Author Manuscript Author Manuscript

vital with the emerging nanotechnology industry and growing potential for human and environmental exposures due to commercial use.

It is generally accepted that dispersants and surfactants form weak associations with the nanoparticles, essentially adsorbing to them and forming dynamic, biomolecular "coronas" (Bihari et al. 2008; Ji et al. 2010; Nel et al. 2009; Pegueroles et al. 2012; Ruh et al. 2012; Sager et al. 2007; Shi et al. 2012; Walczyk et al. 2010; Xia et al. 2012). The coronas are largely determined by the types of nanoparticles and proteins present, and the length of time that they interact. Shi et al. reported that TiO_2 nanobelts with small diameters (~20 nm) adsorb less serum albumin (2012), a primary component of the Porter dispersion media we used, than nanobelts with large diameters (~200 nm). The inflammatory response elicited by the 10 nm TiO_2-NB in our study may have resulted from relatively greater "visibility" of TiO_2-NB in the lung than TiO_2-P5 and TiO_2-A. Indeed, according to Walczyk et al., naked nanoparticles have higher nonspecific affinities for the cell surface than coronated nanoparticles (2010). According to previous studies, surface chemistry (Warheit, Webb, Colvin, et al. 2007; Warheit, Webb, Reed, et al. 2007) and contact area (Hsiao and Huang 2011) between a nanoparticle and a single cell may actually be more important to toxicity than total specific surface area. TiO_2-NB were also found stuck in alveolar septa (Figure 10, left and middle). Still, ICP-MS showed less TiO_2-NB in the lung lobes than TiO_2-P25 or TiO_2-A. This may be due to the relatively higher aerodynamic diameter of TiO_2-NB, which could cause it to deposit higher in the respiratory tract and clear via mucociliary elimination (Figure 10, right).

Based on our results, we believe that future studies should focus on dose metrics to aid in streamlining engineered nanomaterials hazard identification and risk assessments. Nano-scale hyperspectral imaging would allow for accurate histological quantitation of TiO_2 without the complications of tissue digestion or interference of fluorescent/radio-labels.

ACKNOWLEDGEMENTS

Support for this research was provided by:

- University of California, Davis Atmospheric Aerosols and Health Lead Campus Program (aah.ucdavis.edu),
- NIEHS Nano Grand Opportunities (NanoGO) Challenge Grants (RC1 ES018232, and RC2 DE-FG02-08ER64613)
- NIEHS 1U01ES020127-01, Engineered Nanomaterials: Linking Physical and Chemical Properties to Biology.
- Pacific Northwest National Laboratory is operated by Battelle Memorial Institute for the U.S. Department of Energy under Contract Number DE-AC05-76RL01830.

We wish to thank Imelda Espiritu, Katherine Johnson, Amy Madl, Dipti Munshi, Leng Mut, Janice Peake, Laurel Plummer, Vish Seshachellam, Esther Shin, and Dale Uyeminami for technical assistance and Drs. Ting Guo, Angie Louie, Otto Raabe, and Laura Van Winkle for insightful discussions during the course of this study, as well as Suzette Smiley-Jewell for manuscript preparation.

The writing of the article was the sole responsibility of the authors. It has not been published and/or submitted simultaneously for publication elsewhere.

Author Manuscript Author Manuscript Author Manuscript Author Manuscript

ABBREVIATIONS

BALF	Bronchoalveolar Lavage Fluid
BET	Bunauer, Emmett, & Teller
DM	Dispersion Media
DPPC	Dipalmitoylphosphatidylcholine
DSPC	Distearoylphosphatidylcholine
ENM	Engineered Nanomaterial
FLAR	Flame Aerosol Reactor
ICP-MS	Inductively-Coupled Mass Spectrometry
ICP-OES	Inductively-Coupled Optical Emission Spectrometry
IACUC	Institutional Animal Care and Use Committee
IARC	International Agency for Research on Cancer
LDH	Lactate Dehydrogenase
LOEL	Lowest Observed Effect Level
RSA	Rat Serum Albumin
SEM	Scanning Electron Microscopy
TiO_2	Titanium Dioxide
TEM	Transmission Electron Microscopy

REFERENCES

1. Bermudez E, Mangum JB, Wong BA, Asgharian B, Hext PM, Warheit DB, Everitt JI. Pulmonary responses of mice, rats, and hamsters to subchronic inhalation of ultrafine titanium dioxide particles. Toxicological Sciences. 2004; 77(2):347–357. [PubMed: 14600271]
2. Bihari P, Vippola M, Schultes S, Praetner M, Khandoga AG, Reichel CA, Coester C, Tuomi T, Rehberg M, Krombach F. Optimized dispersion of nanoparticles for biological in vitro and in vivo studies. Part Fibre Toxicol. 2008; 5:14. [PubMed: 18990217]
3. Bonner JC. Nanoparticles as a potential cause of pleural and interstitial lung disease. Proc. Am. Thorac. Soc. 2010; 7(2):138–141. [PubMed: 20427587]
4. Bonner JC, Silva RM, Taylor AJ, Brown JM, Hilderbrand SC, Castranova V, Porter D, Elder A, Oberdorster G, Harkema JR, Bramble LA, Kavanagh TJ, Botta D, Nel A, Pinkerton KE. Interlaboratory Evaluation of Rodent Pulmonary Responses to Engineered Nanomaterials: The NIEHS NanoGo Consortium. Environ Health Perspect. 2013
5. Cui YL, Liu HT, Ze YG, Zhang ZL, Hu YY, Cheng Z, Cheng J, Hu RP, Gao GD, Wang L, Tang M, Hong FS. Gene Expression in Liver Injury Caused by Long-term Exposure to Titanium Dioxide Nanoparticles in Mice. Toxicological Sciences. 2012; 128(1):171–185. [PubMed: 22539623]
6. Donaldson K, Murphy F, Schinwald A, Duffin R, Poland CA. Identifying the pulmonary hazard of high aspect ratio nanoparticles to enable their safety-by-design. Nanomedicine. 2011; 6(1):143–156. [PubMed: 21182425]
7. Hamilton RF, Wu NQ, Porter D, Buford M, Wolfarth M, Holian A. Particle length-dependent titanium dioxide nanomaterials toxicity and bioactivity. Particle and Fibre Toxicology. 2009; 6

Author Manuscript Author Manuscript Author Manuscript Author Manuscript

8. Horie M, Fukui H, Endoh S, Maru J, Miyauchi A, Shichiri M, Fujita K, Niki E, Hagihara Y, Yoshida Y, Morimoto Y, Iwahashi H. Comparison of acute oxidative stress on rat lung induced by nano and fine-scale, soluble and insoluble metal oxide particles: NiO and TiO2. Inhalation Toxicology. 2012; 24(7):391–400. [PubMed: 22642288]

9. Hougaard KS, Jackson P, Jensen KA, Sloth JJ, Loschner K, Larsen EH, Birkedal RK, Vibenholt A, Boisen AMZ, Wallin H, Vogel U. Effects of prenatal exposure to surface-coated nanosized titanium dioxide (UV-Titan). A study in mice. Particle and Fibre Toxicology. 2010; 7

10. Hsiao IL, Huang YJ. Effects of various physicochemical characteristics on the toxicities of ZnO and TiO2 nanoparticles toward human lung epithelial cells. Science of the Total Environment. 2011; 409(7):1219–1228. [PubMed: 21255821]

11. Ji ZX, Jin X, George S, Xia TA, Meng HA, Wang X, Suarez E, Zhang HY, Hoek EMV, Godwin H, Nel AE, Zink JI. Dispersion and Stability Optimization of TiO2 Nanoparticles in Cell Culture Media. Environmental Science & Technology. 2010; 44(19):7309–7314. [PubMed: 20536146]

12. Kuhlbusch TAJ, Asbach C, Fissan H, Gohler D, Stintz M. Nanoparticle exposure at nanotechnology workplaces: A review. Particle and Fibre Toxicology. 2011; 8

13. Ma-Hock L, Burkhardt S, Strauss V, Gamer A, Wiench K, van Ravenzwaay B, Landsiedel R. Development of a Short-Term Inhalation Test in the Rat Using Nano-Titanium Dioxide as a Model Substance. Inhalation Toxicology. 2009; 21(2):102–118. [PubMed: 18800274]

14. McKinney W, Jackson M, Sager TM, Reynolds JS, Chen BT, Afshari A, Krajnak K, Waugh S, Johnson C, Mercer RR, Frazer DG, Thomas TA, Castranova V. Pulmonary and cardiovascular responses of rats to inhalation of a commercial antimicrobial spray containing titanium dioxide nanoparticles. Inhalation Toxicology. 2012; 24(7):447–457. [PubMed: 22642294]

15. Meena R, Rani M, Pal R, Rajamani P. Nano-TiO2-Induced Apoptosis by Oxidative Stress-Mediated DNA Damage and Activation of p53 in Human Embryonic Kidney Cells. Applied Biochemistry and Biotechnology. 2012; 167(4):791–808. [PubMed: 22614867]

16. Nel AE, Madler L, Velegol D, Xia T, Hoek EMV, Somasundaran P, Klaessig F, Castranova V, Thompson M. Understanding biophysicochemical interactions at the nano-bio interface. Nature Materials. 2009; 8(7):543–557.

17. Nemmar A, Melghit K, Ali BH. The acute proinflammatory and prothrombotic effects of pulmonary exposure to rutile TiO2 nanorods in rats. Experimental Biology and Medicine. 2008; 233(5):610–619. [PubMed: 18375825]

18. Oberdorster G. Toxicology of ultrafine particles: in vivo studies. Philosophical Transactions of the Royal Society of London Series a-Mathematical Physical and Engineering Sciences. 2000; 358(1775):2719–2739.

19. Oberdorster G, Ferin J, Gelein R, Soderholm SC, Finkelstein J. ROLE OF THE ALVEOLAR MACROPHAGE IN LUNG INJURY - STUDIES WITH ULTRAFINE PARTICLES. Environmental Health Perspectives. 1992; 97:193–199. [PubMed: 1396458]

20. Oberdorster G, Ferin J, Lehnert BE. CORRELATION BETWEEN PARTICLE-SIZE, IN-VIVO PARTICLE PERSISTENCE, AND LUNG INJURY. Environmental Health Perspectives. 1994; 102:173–179. [PubMed: 7882925]

21. Ohtani B, Prieto-Mahaney OO, Li D, Abe R. What is Degussa (Evonik) P25? Crystalline composition analysis, reconstruction from isolated pure particles and photocatalytic activity test. Journal of Photochemistry and Photobiology A : Chemistry. 2010; 216(2–3):179–182.

22. Pegueroles M, Tonda-Turo C, Planell JA, Gil FJ, Aparicio C. Adsorption of Fibronectin, Fibrinogen, and Albumin on TiO2: Time-Resolved Kinetics, Structural Changes, and Competition Study. Biointerphases. 2012; 7(1–4)

23. Porter D, Sriram K, Wolfarth M, Jefferson A, Schwegler-Berry D, Andrew M, Castranova V. A biocompatible medium for nanoparticle dispersion. Nanotoxicology. 2008; 2(3):144–154.

24. Rehn B, Seiler F, Rehn S, Bruch J, Maier M. Investigations on the inflammatory and genotoxic lung effects of two types of titanium dioxide: untreated and surface treated. Toxicology and Applied Pharmacology. 2003; 189(2):84–95. [PubMed: 12781626]

25. Renwick LC, Brown D, Clouter A, Donaldson K. Increased inflammation and altered macrophage chemotactic responses caused by two ultrafine particle types. Occupational and Environmental Medicine. 2004; 61(5):442–447. [PubMed: 15090666]

Author Manuscript Author Manuscript Author Manuscript Author Manuscript

26. Robichaud CO, Uyar AE, Darby MR, Zucker LG, Wiesner MR. Estimates of Upper Bounds and Trends in Nano-TiO2 Production As a Basis for Exposure Assessment. Environmental Science & Technology. 2009; 43(12):4227–4233. [PubMed: 19603627]
27. Ruh H, Kuhl B, Brenner-Weiss G, Hopf C, Diabate S, Weiss C. Identification of serum proteins bound to industrial nanomaterials. Toxicology Letters. 2012; 208(1):41–50. [PubMed: 22001751]
28. Saber AT, Jacobsen NR, Mortensen A, Szarek J, Jackson P, Madsen AM, Jensen KA, Koponen IK, Brunborg G, Gutzkow KB, Vogel U, Wallin H. Nanotitanium dioxide toxicity in mouse lung is reduced in sanding dust from paint. Particle and Fibre Toxicology. 2012; 9
29. Saber AT, Jensen KA, Jacobsen NR, Birkedal R, Mikkelsen L, Moller P, Loft S, Wallin H, Vogel U. Inflammatory and genotoxic effects of nanoparticles designed for inclusion in paints and lacquers. Nanotoxicology. 2012; 6(5):453–471. [PubMed: 21649461]
30. Sager TM, Kommineni C, Castranova V. Pulmonary response to intratracheal instillation of ultrafine versus fine titanium dioxide: role of particle surface area. Particle and Fibre Toxicology. 2008; 5
31. Sager TM, Porter DW, Robinson VA, Lindsley WG, Schwegler-Berry DE, Castranova V. Improved method to disperse nanoparticles for in vitro and in vivo investigation of toxicity. Nanotoxicology. 2007; 1(2):118–129.
32. Shi J, Feng B, Lu X, Weng J. Adsorption of bovine serum albumin onto titanium dioxide nanotube arrays. International Journal of Materials Research. 2012; 103(7):889–896.
33. Shimizu M, Tainaka H, Oba T, Mizuo K, Umezawa M, Takeda K. Maternal exposure to nanoparticulate titanium dioxide during the prenatal period alters gene expression related to brain development in the mouse. Particle and Fibre Toxicology. 2009; 6
34. Stoeger T, Reinhard C, Takenaka S, Schroeppel A, Karg E, Ritter B, Heyder J, Schulz H. Instillation of six different ultrafine carbon particles indicates a surface area threshold dose for acute lung inflammation in mice. Environmental Health Perspectives. 2006; 114(3):328–333. [PubMed: 16507453]
35. Takeda K, Suzuki KI, Ishihara A, Kubo-Irie M, Fujimoto R, Tabata M, Oshio S, Nihei Y, Ihara T, Sugamata M. Nanoparticles Transferred from Pregnant Mice to Their Offspring Can Damage the Genital and Cranial Nerve Systems. Journal of Health Science. 2009; 55(1):95–102.
36. Walczyk D, Bombelli FB, Monopoli MP, Lynch I, Dawson KA. What the Cell "Sees" in Bionanoscience. Journal of the American Chemical Society. 2010; 132(16):5761–5768. [PubMed: 20356039]
37. Warheit DB, Webb TR, Colvin VL, Reed KL, Sayes CR. Pulmonary bioassay studies with nanoscale and fine-quartz particles in rats: Toxicity is not dependent upon particle size but on surface characteristics. Toxicological Sciences. 2007; 95(1):270–280. [PubMed: 17030555]
38. Warheit DB, Webb TR, Reed KL, Frerichs S, Sayes CM. Pulmonary toxicity study in rats with three forms of ultrafine-TiO2 particles: Differential responses related to surface properties. Toxicology. 2007; 230(1):90–104. [PubMed: 17196727]
39. Warheit DB, Webb TR, Sayes CM, Colvin VL, Reed KL. Pulmonary instillation studies with nanoscale TiO2 rods and dots in rats: Toxicity is not dependent upon particle size and surface area. Toxicological Sciences. 2006; 91(1):227–236. [PubMed: 16495353]
40. Weir A, Westerhoff P, Fabricius L, Hristovski K, von Goetz N. Titanium Dioxide Nanoparticles in Food and Personal Care Products. Environmental Science & Technology. 2012; 46(4):2242–2250. [PubMed: 22260395]
41. Weir, Alex. TiO2 Nanomaterials: Human Exposure and Environmental Release, Arizona State University. 2011
42. Xia T, Hamilton RF Jr, Bonner JC, Crandall ED, Elder A, Fazlollahi F, Girtsman TA, Kim K, Mitra S, Ntim SA, Orr G, Tagmount M, Taylor AJ, Telesca D, Tolic A, Vulpe CD, Walker AJ, Wang X, Witzmann FA, Wu N, Xie Y, Zink JI, Nel A, Holian A. Interlaboratory Evaluation of in Vitro Cytotoxicity and Inflammatory Responses to Engineered Nanomaterials: The NIEHS Nano Go Consortium. Environmental Health Perspectives. 2012
43. Xia T, Malasarn D, Lin S, Ji Z, Zhang H, Miller RJ, Keller AA, Nisbet RM, Harthorn BH, Godwin HA, Lenihan HS, Liu R, Gardea-Torresdey J, Cohen Y, Madler L, Holden PA, Zink JI, Nel AE.

Author Manuscript Author Manuscript Author Manuscript Author Manuscript

Implementation of a Multidisciplinary Approach to Solve Complex Nano EHS Problems by the UC Center for the Environmental Implications of Nanotechnology. Small. 2012

44. Zhang J, Song W, Guo J, Zhang J, Sun Z, Li L, Ding F, Gao M. Cytotoxicity of different sized TiO2 nanoparticles in mouse macrophages. Toxicol Ind Health. 2012

Author Manuscript Author Manuscript Author Manuscript Author Manuscript

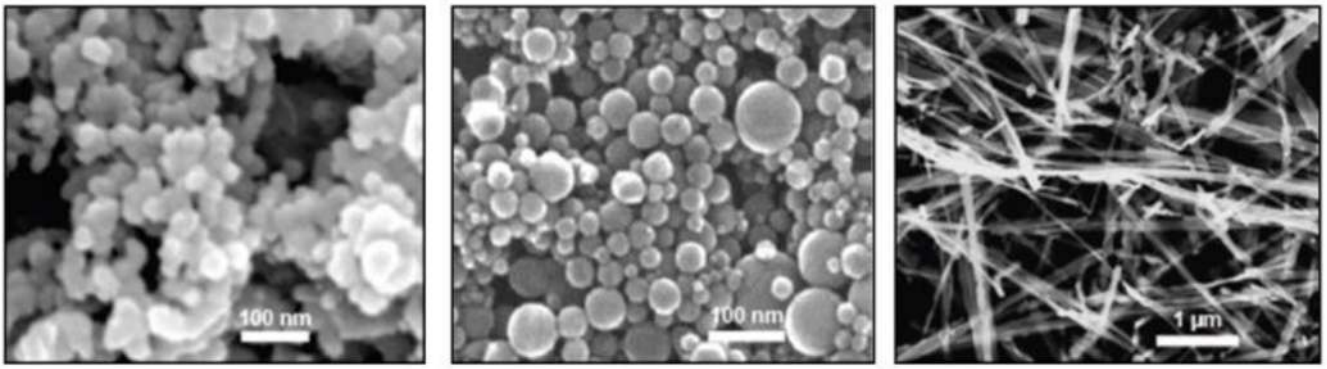

Figure 1. SEM images of all studied nanomaterials in pristine form

From left to right: TiO_2-P25, TiO_2-A, and TiO_2-NB. Spherical particle types, TiO_2-P25 and TiO_2-A, averaged approximately 26 nm in diameter. TiO_2-NB averaged 7000 nm in length and 200 nm in width, and individual nanobelts were approximately 10 nm thick. Scale indicated by the white bars. Reproduced with permission from *Environmental Health Perspectives*.

Author Manuscript Author Manuscript Author Manuscript Author Manuscript

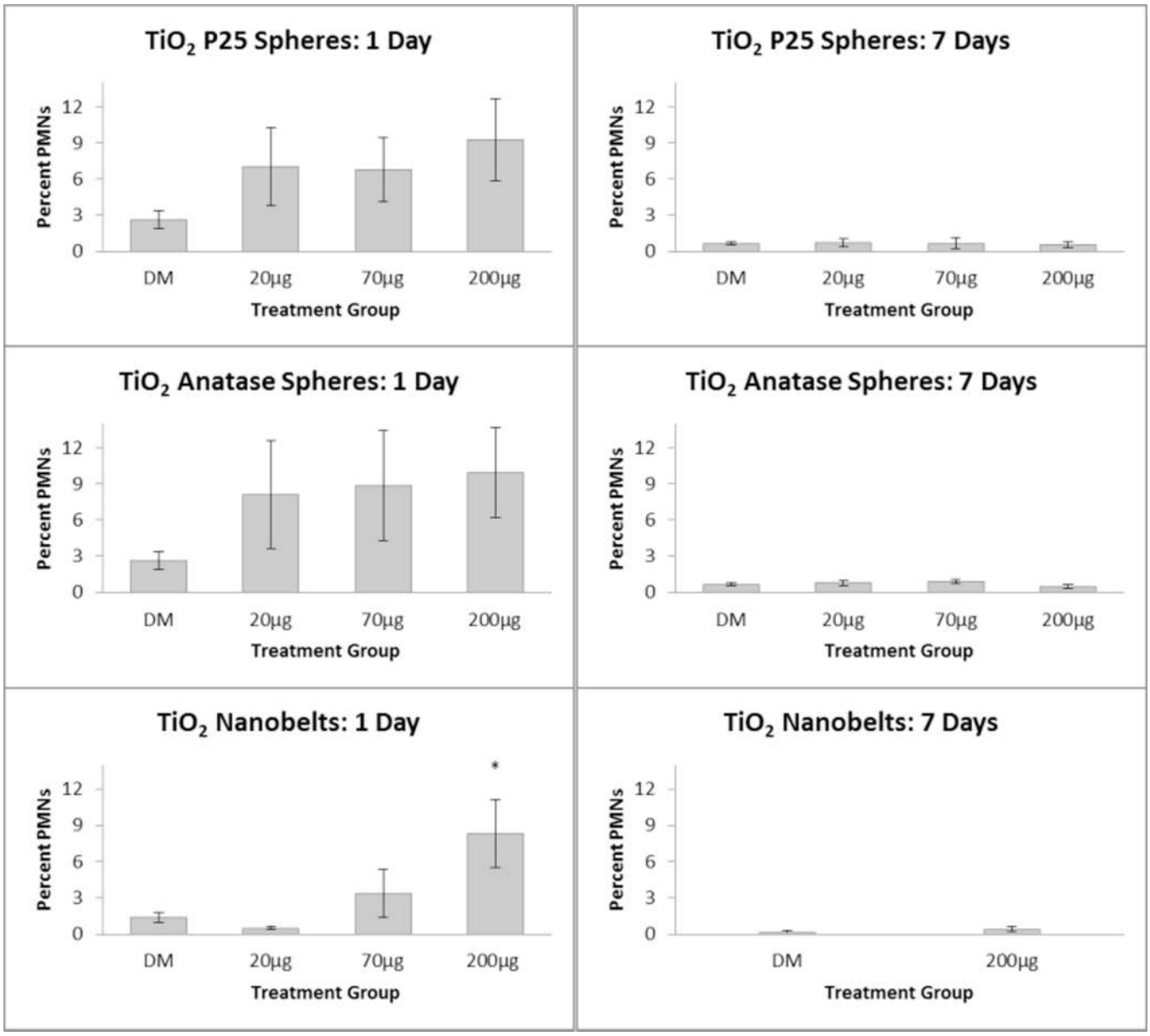

Figure 2. Stimulation of neutrophilic inflammation in the lungs of rats by TiO_2 engineered nanomaterials

Percentages of neutrophils (PMNs) in BALF 1 day (left panels) and 7 days (right panels) after IT exposure to P25 nanospheres (top), anatase nanospheres (middle), or anatase nanobelts (bottom). *P<0.05 compared to DM-exposed controls.

Author Manuscript Author Manuscript Author Manuscript Author Manuscript

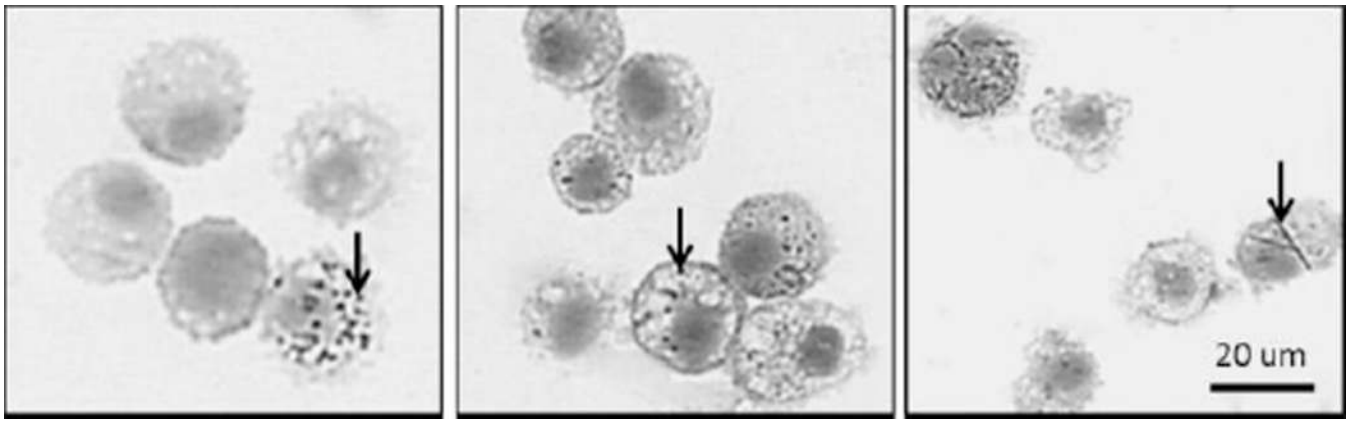

Figure 3. Instilled TiO_2-A causes moderate but sustained particle loading in alveolar macrophages

Cells recovered from BALF at 7 days post exposure to TiO_2-P25 (left), TiO_2-A (middle) and TiO_2-NB (right) by intratracheal instillation. Panels are Phase Contrast microscopy images of representative cells from rats given a single dose of TiO_2. BAL cells were stained with Diff Qwik®. Arrows indicate TiO_2 nanoparticles. Scale indicated by black bar.

Author Manuscript Author Manuscript Author Manuscript Author Manuscript

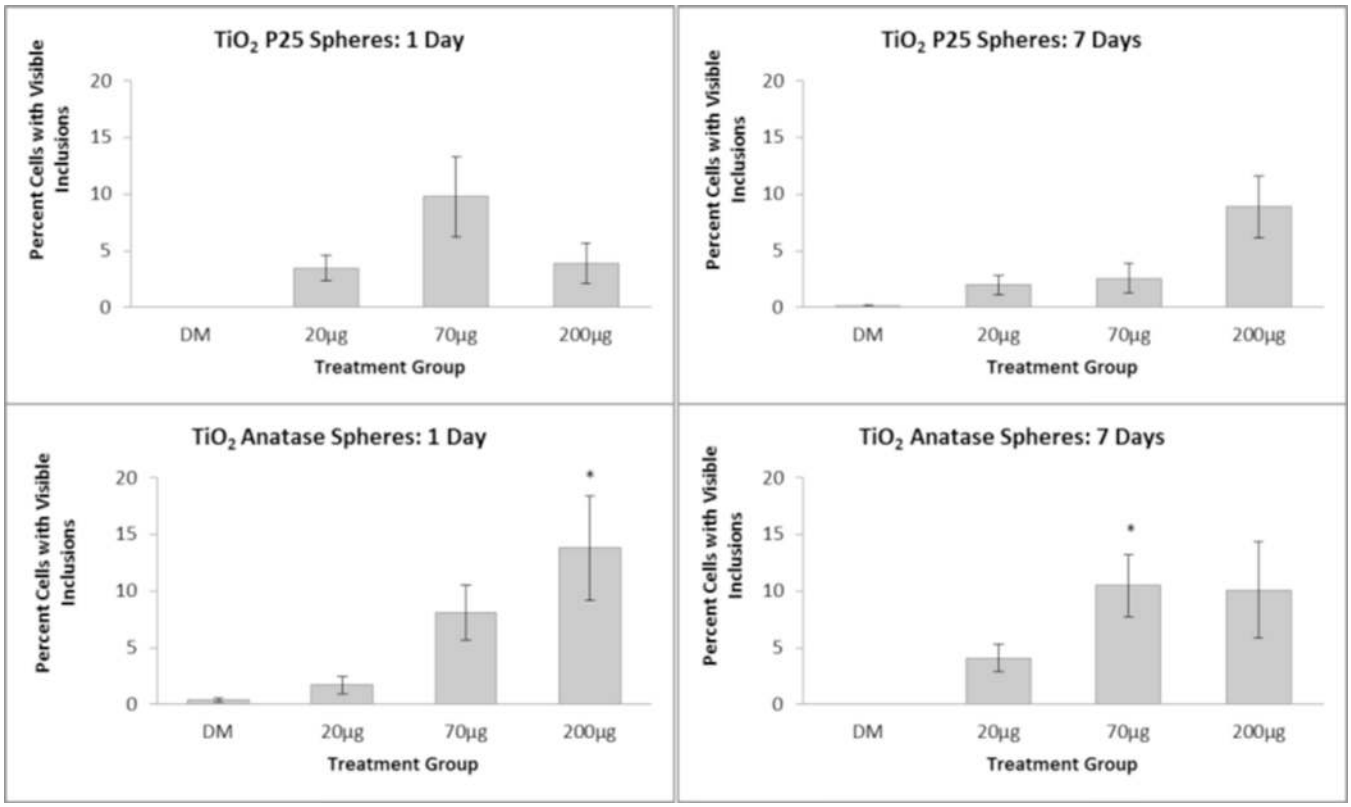

Figure 4. TiO_2 engineered nanomaterials uptake by macrophages in the lungs

Percentages of macrophages in BALF with visible particle inclusions 1 day (left panels) and 7 days (right panels) after intratracheal instillation exposure to TiO_2-P25 nanospheres (top) or TiO_2-A nanospheres (bottom). *P<0.05 compared to DM-exposed controls.

Author Manuscript Author Manuscript Author Manuscript Author Manuscript

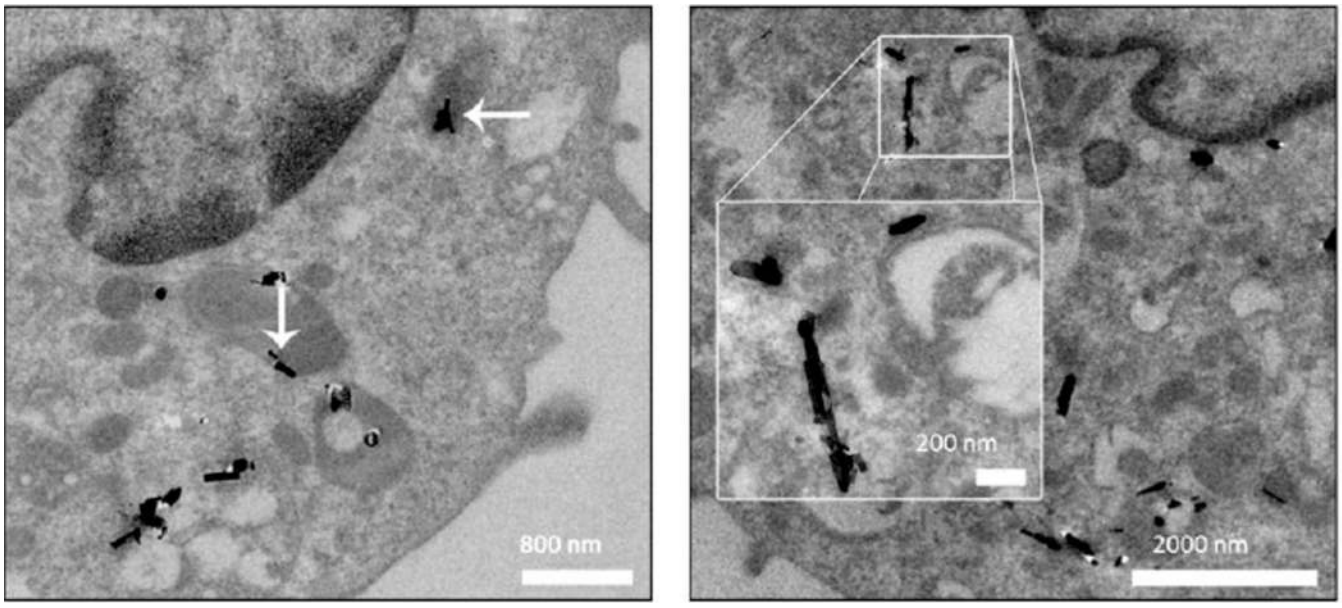

Figure 5. TEM images of TiO_2 nanobelts (TiO_2-NB) in alveolar macrophages

Cells recovered from BALF at 1 (left) and 7 (right) days post instillation. Panels are images of representative cells from rats given 200 μg TiO_2-NB. White arrows indicate TiO_2-NB aggregates. Scale indicated by the white bars.

Author Manuscript Author Manuscript Author Manuscript Author Manuscript

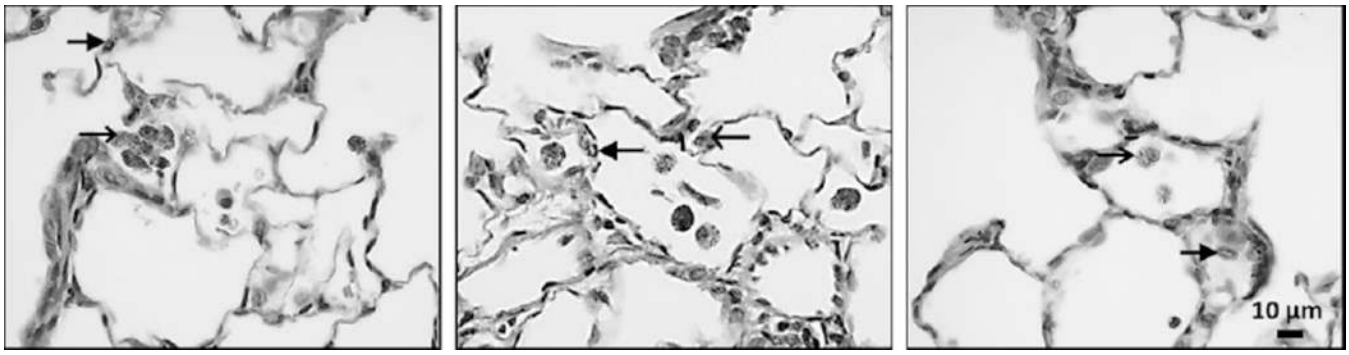

Figure 6. TiO_2 causes inflammatory infiltrates in the left lung at 1 day post exposure

Histopathological findings from exposure to 200 µg/250 µL of TiO_2-P25 (left), TiO_2-A (middle) and TiO_2-NB (right) by intratracheal instillation. Panels are Brightfield microscopy images of representative lung tissues from rats given a single dose of TiO_2. Tissues were stained with hematoxylin and eosin. Closed arrow = inflammatory cell infiltrate; Open arrow = particle laden cells; TB = terminal bronchiole. Scale indicated by black bar.

Author Manuscript Author Manuscript Author Manuscript Author Manuscript

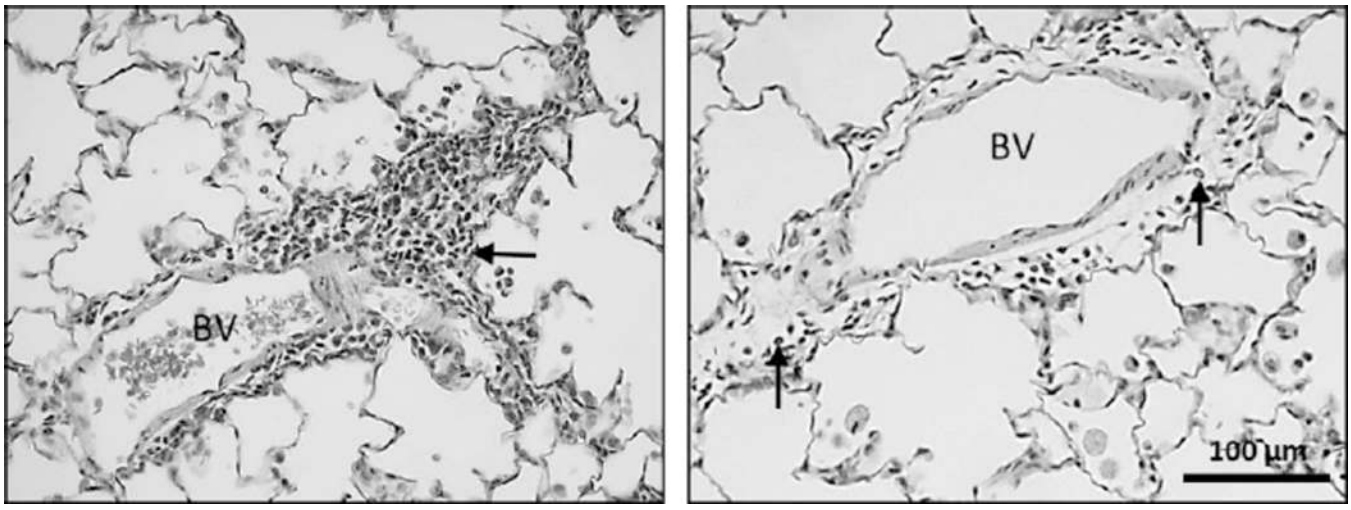

Figure 7. Inflammatory cells can be seen at 1 and 7 days post exposure to TiO_2-NB

Histopathological findings from exposure to 200 µg/250 µL of TiO_2-NB by intratracheal instillation. Panels are Brightfield microscopy images of representative lung tissues from rats given a single dose of TiO_2. Tissues were stained with hematoxylin and eosin. Closed arrow = mixed inflammatory cell infiltrate; BV = blood vessel. Scale indicated by black bar.

Author Manuscript Author Manuscript Author Manuscript Author Manuscript

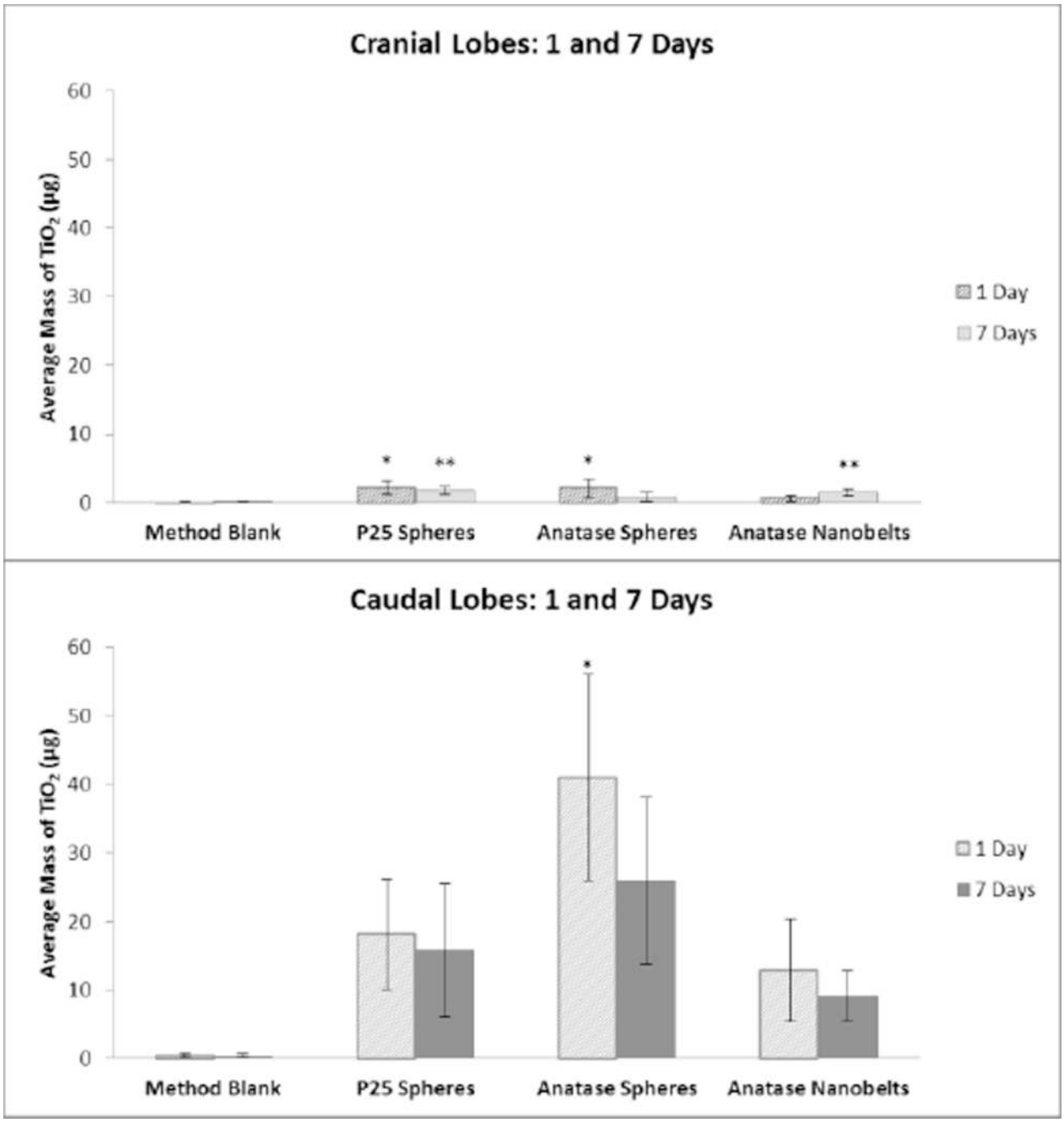

Figure 8. TiO_2 lung burden in the right cranial and caudal lobes

Average mass of TiO_2 observed in the cranial (top panel) and caudal (bottom panel) lung lobes 1 day and 7 days after intratracheal instillation exposure to TiO_2-P25 nanospheres, TiO_2-A nanospheres, or TiO_2-NB. *,**P<0.05 compared to method blank (control) from 1 day and 7 days, respectively.

Author Manuscript Author Manuscript Author Manuscript Author Manuscript

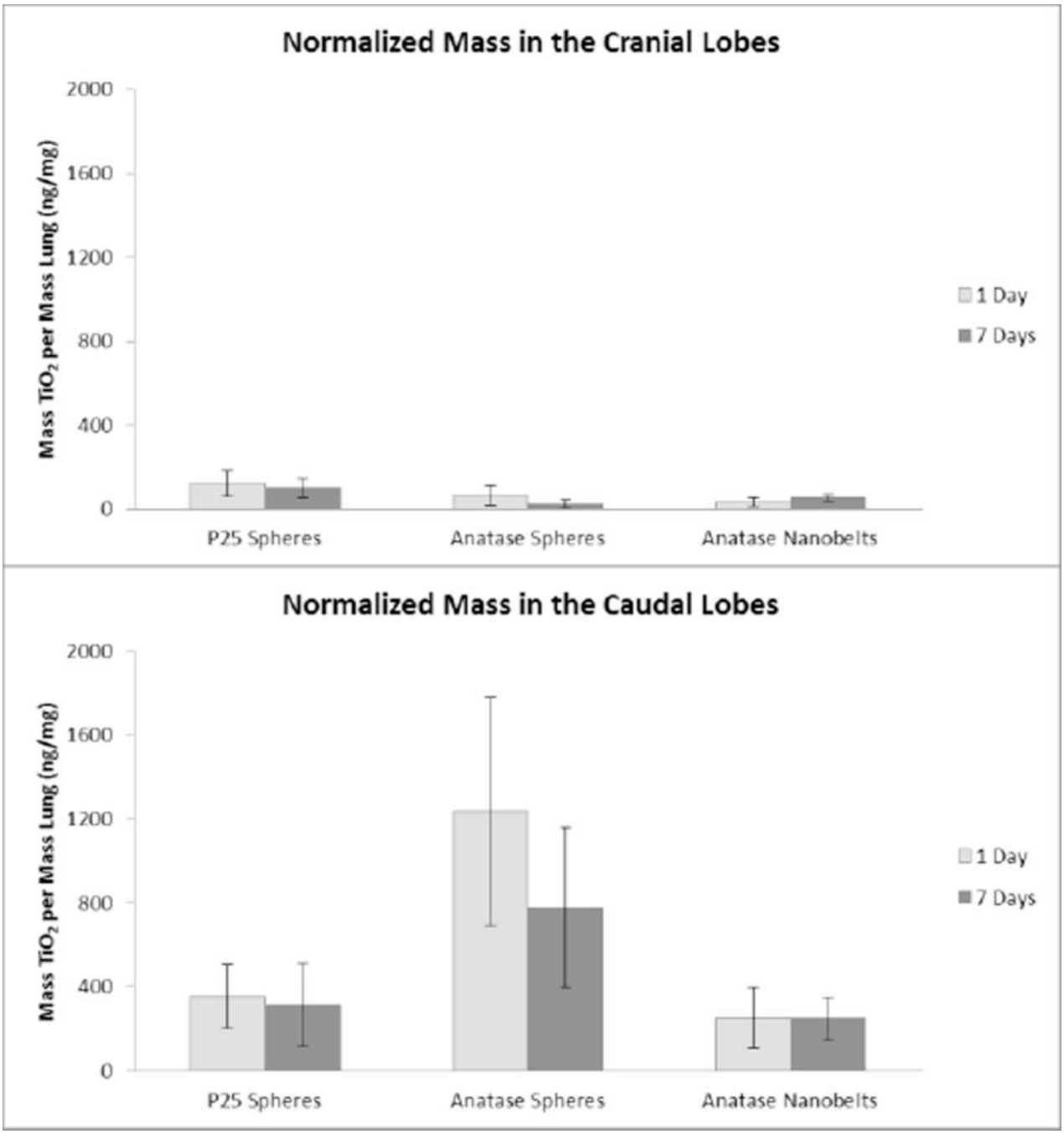

Figure 9. TiO_2 lung burden in the right cranial and caudal lobes normalized by lung mass

Normalized mass of TiO_2 observed in the cranial (top) and caudal (bottom) lung lobes 1 and 7 days after a single IT exposure.

Author Manuscript Author Manuscript Author Manuscript Author Manuscript

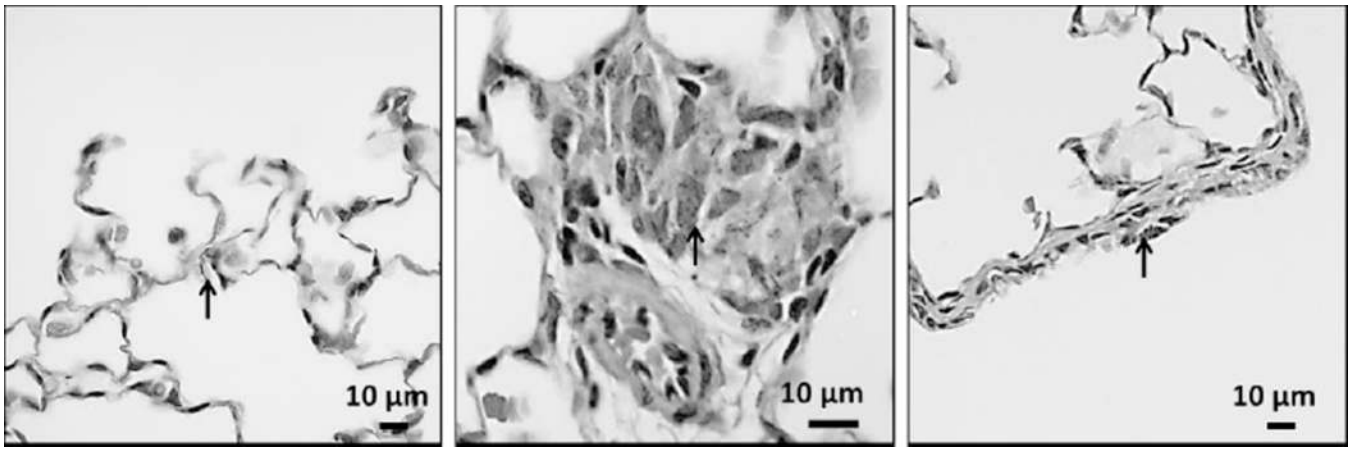

Figure 10. Deep lung penetration of TiO_2 nanobelts at 1 day post exposure

Histopathological findings from exposure to 200 µg/250 µL of TiO_2-NB by intratracheal instillation. Panels are Brightfield microscopy images of representative lung tissues from rats given a single dose of TiO_2. Tissues were stained with hematoxylin and eosin. Open arrow = TiO_2-NB aggregates. Scale indicated by black bar.